JOURNAL OF MOLECULAR SPECTROSCOPY **121**, 380–400 (1987)

Rotation–Vibration Spectrum of HT: Line Position Measurements of the 1–0, 4–0, and 5–0 Bands

MEI-CHEN CHUANG[1] AND RICHARD N. ZARE

Department of Chemistry, Stanford University, Stanford, California 94305

Optoacoustic techniques have been used to determine the line positions of the 1–0 fundamental and 4–0 and 5–0 overtones of the HT ($^1H^3H$) molecule with an accuracy of better than 0.01 cm^{-1}. Comparison with line positions predicted from ab initio calculations that include adiabatic, relativistic, radiative, and nonadiabatic corrections shows disagreement outside of the experimental uncertainties. © 1987 Academic Press, Inc.

I. INTRODUCTION

The separation of nuclear and electronic motions provides the major conceptual framework for describing the energy levels of isolated molecules. In its simplest form called the Born–Oppenheimer approximation (*1*), the positions of the nuclei are clamped and the electronic energy of the system is calculated as a parametric function of the nuclear coordinates. Then the nuclei are allowed to move under the influence of this electronic potential energy function. In a more sophisticated treatment, called the adiabatic approximation (*2*), the concept of a potential energy function is still retained by including the expectation value of the coupling between the electronic and nuclear motions in the electronic potential.

Nonadiabatic effects, however, are known to be significant in a number of diverse phenomena from the description of the radiationless decay of excited electronic states (*3*) to the detailed nature of perturbations (*4*). Often two or more electronic states are in close proximity so that their mutual interaction causes a breakdown in the adiabatic approximation, although it is generally supposed that nonadiabatic effects in the ground electronic states of molecules are quite small and are usually ignored. The hydrogen molecule and its isotopes represent an exception due to the light masses of the nuclei which accentuate nonadiabatic effects. Moreover, the energy levels of H_2, HD, D_2, etc., can be calculated to the highest accuracy of any neutral diatomic system. Thus the experimental determination of the H_2, HD, D_2, etc., ground state energy level structure can be used to test our most profound understanding of the behavior of an isolated molecular system.

Presently, extremely accurate line positions for many transitions in H_2 and some transitions in HD and D_2 are available due to advances in spectroscopic instrumentation, in particular the use of high-resolution Raman spectroscopy (*5*), long path

[1] Present address: Department of Chemistry, University of California, Berkeley, Calif. 94720.

0022-2852/87 $3.00

length absorption (*6–8*), electric field induced absorption (*9*), Fourier transform spectroscopy (*10–13*), laser diode spectroscopy (*14, 15*), and laser stimulated Raman spectroscopy (*16*). In contrast, little work has been done on the line positions for tritium-containing molecular hydrogen, HT, DT, and T_2. In particular, for HT we have only two gas-phase Raman studies (*17, 18*) providing information on the 1–0 fundamental and the pure rotational spectrum. The HT molecule is of particular interest because an accurate determination of its energy level structure would permit a test of how well present theory scales with change in reduced nuclear mass.

Unfortunately, the radioactive decay of the tritium nucleus, ${}^{3}_{1}H \rightarrow {}^{3}_{2}He + {}^{0}_{-1}\beta$ (19 keV), presents severe obstacles in the spectroscopic study of HT. For example, long path length absorption as well as FT–IR measurements appear to be ruled out while the much-more-sensitive laser optoacoustic techniques, which have been applied with success to HD (*19–21*), confront the difficulty that the intimate contact of HT with electric microphones destroys the latter. Like HD, the HT molecule has no dipole moment in the traditional Born–Oppenheimer and adiabatic approximations (*22*), but develops a tiny electric dipole moment as it rotates and vibrates since the electrons do not adjust instantaneously to the positions of the nuclei (*23*). It is this property which is exploited in the present study of HT. We report here the first accurate measurement of the 1–0, 4–0, and 5–0 electric-dipole-allowed rovibrational transitions of HT. This is accomplished with optoacoustic spectroscopy using an optical microphone (optophone) as the detector (*24*) and a mechanically chopped high-resolution tunable laser (a color-center laser for 1–0 and ring dye laser for 4–0 and 5–0) as the excitation source. Comparison with the most accurate nonadiabatic calculation available for HT shows that theory presently is unable to predict the HT line positions within the accuracy of the experiment.

II. EXPERIMENTAL DETAILS

The experimental details of the optophone technique and its comparison with the normal optoacoustic technique have been described elsewhere (*24*). Figure 1 shows the schematic setup of the present experiment. The major difference between the present study and the previous report is the location of the sample cell. Formerly the cell was placed inside the cavity of a linear dye laser, while presently it is placed outside the laser cavity. The reason for this configuration is that single-mode lasers are used in this study and amplitude modulation at any point before or within the single-mode laser will cause mode hops and disturbance of the frequency control electronics. Two passes of the laser beam through the cell are achieved by reflection of the transmitted light with a suitable mirror.

As the wavelength of the excitation laser is tuned, either continuously or by hopping cavity modes, the reflection of a He–Ne laser beam off the pellicle beam splitter (Oriel 3743) situated inside the cell is monitored by a position sensing detector (Silicon Detector Corporation SD-113-24-21-021). The position sensing detector senses the displacement of the pellicle generated by the pressure wave due to HT absorption of the excitation laser beam. This signal is processed by a lock-in amplifier (PAR 186A). The laser power is simultaneously monitored by a power meter (NRC 815) in the visible or by a PbS photoconductive detector in the infrared, and is also processed by

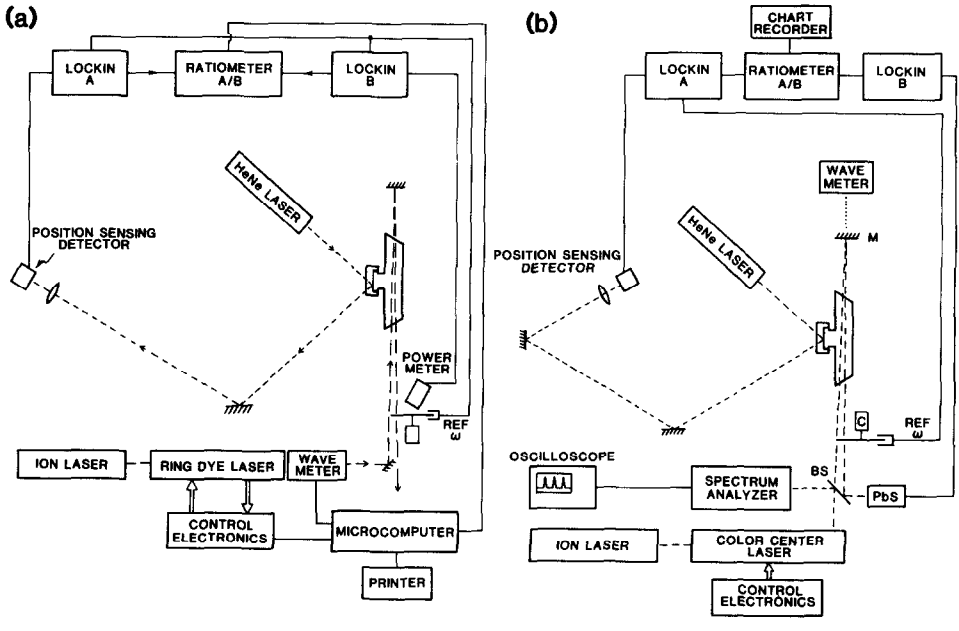

FIG. 1. Schematic diagram of the experimental setup (a) for HT overtone measurements and (b) for the HT fundamental. In the latter, BS = ZnSe beam splitter, PbS = the lead sulfide protoconductive detector, and the laser frequency is measured by removing the mirror M and shutting off the laser beam chopper C.

a lock-in amplifier (PAR 124A). The optophone signal, after normalization (PAR 192 ratiometer) to the laser power, is either displayed on a stripchart recorder (Soltec 1242) or is digitized and stored with a microcomputer (Apple II+).

The optophone cell is very similar to that described in Ref. (*24*) except that there is no electric microphone chamber in the present cell. Quartz windows are used in the visible and CaF_2 windows in the IR.

For the two vibrational overtone bands in the visible region, a Coherent 699-29 microcomputer-controlled ring dye laser is used. The 4–0 band is covered by LD-700 dye (Exciton Corp.) pumped by the all red lines output (4W) from a krypton ion laser (Spectra-Physics 171-01); the 5–0 band is spanned by DCM dye (Exciton Corp.) pumped by the 514-nm output from an argon ion laser (Spectra-Physics 171-18). Typical output power of the LD-700 in the 4–0 band region varies from 350 to 600 mW. The rapidly decreasing laser power toward longer wavelength prevents us from recording more *P*-branch transitions. In the 5–0 band region, the laser power ranges from 600 to 800 mW. The nominal resolution of the ring dye laser is 1 MHz (3×10^{-5} cm^{-1}).

The absolute accuracy of the wavemeter equipped with the ring dye laser is better than 4 parts in 10^7, which translates to better than 5×10^{-3} cm^{-1} for the 4–0 band and better than 6×10^{-3} cm^{-1} for the 5–0 band. The wavemeter is calibrated against the neon optogalvanic signal of a hollow cathode lamp (Perkin-Elmer). The calibration was performed separately for the 4–0 band and for the 5–0 band with the vacuum line positions published by Crosswhite (*25*) as the standard. When neon transitions

other than those used for calibration were measured, the maximum deviation from the literature value was ± 0.003 cm^{-1}.

To check further the accuracy of the wavemeter, the 4–0 band of HD was measured. The wavelength region of this band falls between the 4–0 and 5–0 bands of HT. Five rovibrational transitions were recorded. The deviations of our results from the reported values by McKellar *et al.* (*7*) after correction for a pressure shift (*7*) of -0.010 cm^{-1} per amagat are well within the quoted experimental error of Ref. (*7*). Thus, we believe the absolute accuracy of the wavemeter itself is ± 0.003 cm^{-1}.

For each rovibrational transition in the overtone, a continuous 20-GHz scan sweeps through the line. The scan starts roughly at 10 GHz below the peak frequency and ends at approximately 10 GHz above. This is sufficient to cover the entire pressure broadened line (3–4 GHz FWHM). A peak finding routine included in the dye laser control software (Coherent 699-29) locates the peak position by identifying the zero crossing point in the first derivative of the spectrum.

For the measurement of the 1–0 band, the light source is a single-mode color-center laser (Burleigh FCL-20) pumped by the all red lines output (1.2 W) of a krypton ion laser (Spectra-Physics 171-01). The output of the lithium-doped RbCl crystal covers the entire 1–0 band region with an output power of ~ 15 mW and a resolution of 1 MHz. The frequency measurement is accomplished using another wavemeter (Burleigh WA-20-IR). The accuracy of the wavemeter is 1 part in 10^6, which is equivalent to better than 0.004 cm^{-1} in the wavelength region of interest, but the display of the wavemeter in the frequency scale rounds off the reading to 0.01 cm^{-1}. The wavemeter is also checked against known HD fundamental transitions (*13*). It always reproduces the first two digits after the decimal point with the third digit rounded off.

The scan through each fundamental transition is achieved by hopping cavity modes of the color center laser in steps of 0.01 cm^{-1}. A generator producing a 150-V ramp causes the intracavity etalon to hop 20 cavity modes. This 6-GHz-wide scan is fully sufficient to cover the 900-MHz FWHM lines in the 1–0 band. During each scan, a small fraction of the laser beam is reflected into a spectrum analyzer (Burleigh FCL-975). The output of the spectrum analyzer is displayed on an oscilloscope. Whenever a mode hop occurs, a tick mark is made manually on the spectrum displayed by the stripchart recorder. Slight nonlinearity is observed in each scan, but this does not affect the accuracy of the transition frequency determination.

The peak of each transition is located by tuning the ramp voltage manually. When the peak is found, the frequency of the laser is measured with the wavemeter. This requires the chopper to be stopped and the reflection mirror to be removed (see Fig. 1b). Due to the nature of the mode hop scan, the peak position determined this way may not be the true peak position, but obviously the true position must fall within ± 0.005 cm^{-1} of the mode-hopped peak position.

The HT sample is obtained from Lawrence Livermore National Laboratory as an equilibrium mixture of H_2, T_2, and HT with very small amounts of He, HD, and D_2 impurities, as determined from mass spectrometry. H_2 gas is added to the sample to increase the acoustic coupling between the HT and the pellicle. This practice may also shift the equilibrium to give more HT by consuming T_2. The estimated HT partial pressure is 166 Torr (600 Torr total pressure) in the two overtone bands and is 83

Torr (300 Torr total pressure) in the fundamental band, assuming the gas mixture completely reached equilibrium.

Minor water vapor desorbed from the cell wall is the only impurity observed in the spectrum. For most of the transitions, this does not cause any problem. Whenever there is ambiguity due to a nearby water transition, a water spectrum is taken to remove any uncertainty regarding the identification of the HT transition. Fortunately, no serious overlap occurs in all the lines observed which would interfere with the HT line position measurement.

III. RESULTS

Seven transitions are observed in the 1–0 band, and six transitions are observed in each of the two overtone bands. Figures 2–4 present all the measured lines. The notation

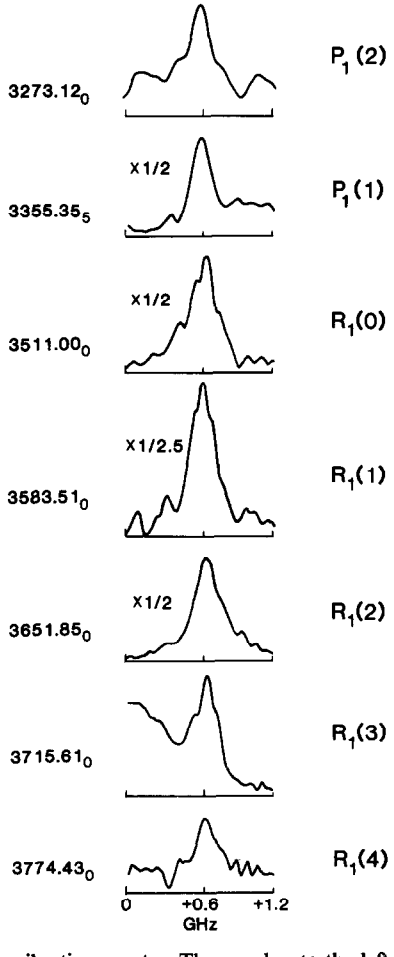

FIG. 2. The HT 1–0 rotation–vibration spectra. The number to the left of each spectrum indicates the frequency (cm^{-1}) at the starting point of the trace. The scale at the bottom of each spectrum is relative to this frequency.

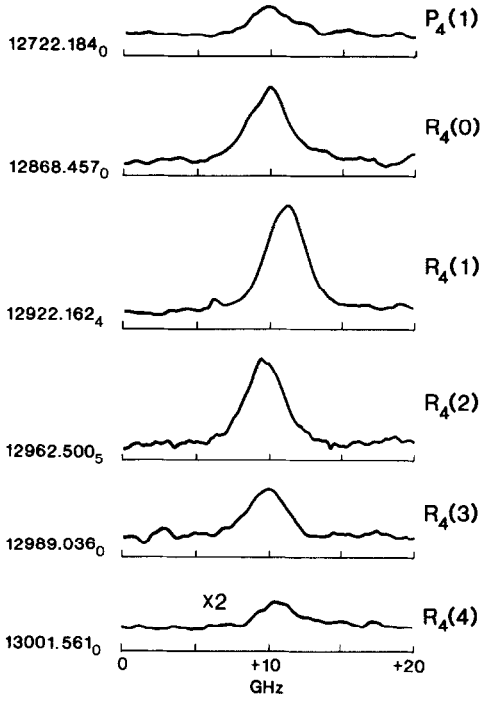

FIG. 3. HT 4–0 rotation–vibration spectra. The number to the left of each spectrum indicates the frequency (cm^{-1}) at the starting point of the trace. The scale at the bottom of each spectrum is relative to this frequency.

is standard: P and R indicate $\Delta J = -1$ and $\Delta J = +1$ transitions, respectively; the upper state vibrational quantum number appears as a subscript on the branch designation (all the transitions originate from the ground vibrational state, $v'' = 0$); the lower state rotational quantum number J'' is given in parentheses following the branch designation.

Table I lists the transition frequencies of all the observed lines without correction for pressure shift. The error limits in parentheses are estimated as follows: A large contribution to the noise in the 1–0 band comes from the stepwise nature of the mode hop scan. Nevertheless, this does not increase the error in the determination of the transition frequency because as long as the peak can be found without ambiguity, as is the case, the only contribution to the error is the combined uncertainty introduced by the wavemeter and the nature of the mode hop scan, which is ± 0.01 cm^{-1}. For the 4–0 and 5–0 bands, however, a lower signal-to-noise ratio does cause uncertainty in locating the peak position. Such uncertainty compounded with the intrinsic error of the wavemeter gives an estimated error of ± 0.005 cm^{-1} for stronger lines and ± 0.010 cm^{-1} for weaker lines. These error limits are confirmed by repeating the measurements.

The consistency of our measurements is further checked by comparing the two combination differences, $R_5(0) - P_5(2)$ and $R_1(0) - P_1(2)$. The former is 237.866 $\pm$ 0.015 cm^{-1} while the latter is 237.880 $\pm$ 0.020 cm^{-1}. The agreement is quite satisfactory.

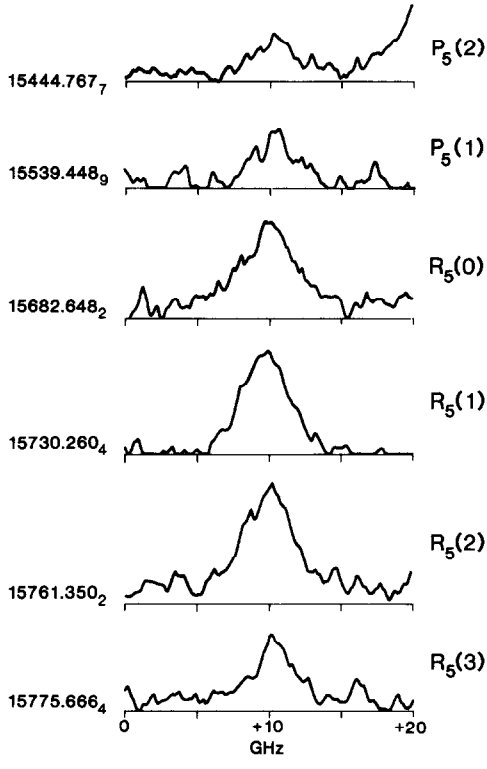

FIG. 4. HT 5–0 rotation–vibration spectra. The number to the left of each spectrum indicates the frequency (cm^{-1}) at the starting point of the trace. The scale at the bottom of each spectrum is relative to this frequency.

The pressure shifts of a number of HD transitions have been measured (*21, 28, 29*) and can be used to estimate those for HT. If we assume that the pressure shifts of the HT transitions are the same as those of HD, the pressure shift coefficients of *pure* HT for the 1–0, 4–0, and 5–0 bands should be −0.0023, −0.0092, and −0.0115 cm^{-1} $amagat^{-1}$, respectively.

If our sample were pure HT, the pressure shifts are calculated to be −0.0009, −0.0072, and −0.0091 cm^{-1} for the 1–0, 4–0, and 5–0 bands, respectively, which are on the order of the line position uncertainties. In reality, the sample is predominantly a mixture of HT and H_2 with the ratio of 1:3. One would expect the pressure shifts of the mixture to be *even smaller* than those of pure HT due to the smaller interaction between HT and H_2. Consequently, we have chosen to ignore the pressure shifts in the HT line positions, although such shifts are certainly present and cause the transition frequencies to be systematically smaller than at zero pressure. Such a systematic error affects primarily the band origins rather than the rotational dependence of the energy level structure.

A least-squares fit reproduces the observed line positions to an rms deviation of 0.005 cm^{-1}. The energy expression is assumed to be

TABLE I

Observed and Calculated HT Line Positions

Transition	Observed [a] (cm^{-1})	Calculated [b] (cm^{-1})	Residual (cm^{-1})
	1-0 Band		
$P_1(2)$	3273.140(10)	3273.145	-0.005
$P_1(1)$	3355.355(10)	3355.353	+0.002
$R_1(0)$	3511.020(10)	3511.022	-0.002
$R_1(1)$	3583.530(10)	3583.526	+0.004
$R_1(2)$	3651.870(10)	3651.868	+0.002
$R_1(3)$	3715.630(10)	3715.634	-0.004
$R_1(4)$	3774.450(10)	3774.451	-0.001
	4-0 Band		
$P_4(1)$	12722.515(7)	12722.512	+0.003
$R_4(0)$	12868.786(5)	12868.786	+0.000
$R_4(1)$	12922.534(5)	12922.534	+0.000
$R_4(2)$	12962.825(5)	12962.831	-0.006
$R_4(3)$	12989.369(5)	12989.367	+0.002
$R_4(4)$	13001.917(7)	13001.915	+0.002
	5-0 Band		
$P_5(2)$	15445.118(10)	15445.113	+0.005
$P_5(1)$	15539.796(10)	15539.798	-0.002
$R_5(0)$	15682.984(5)	15682.990	-0.006
$R_5(1)$	15730.589(5)	15730.587	+0.002
$R_5(2)$	15761.691(5)	15761.686	+0.005
$R_5(3)$	15776.009(10)	15776.014	-0.005

a) The error estimation is given in the text.
b) Based on a least-squares fit using the molecular constants given in Table II.

$$E(v,J)=\nu_v+B_vJ(J+1)-D_v[J(J+1)]^2+H_v[J(J+1)]^3, \tag{1}$$

where

$$D_v=D_e+\beta_e(v+\tfrac{1}{2}), \tag{2}$$

and

$$H_v=H_e, \tag{3}$$

and all energy levels are measured relative to $E(0, 0) = \nu_0$, which is taken to be the zero reference energy. The transition frequencies for P- and R-branch lines are

$$\nu_P(v,J-1;0,J)=E(v,J-1)-E(0,J), \tag{4}$$

and

$$\nu_R(v,J+1;0,J)=E(v,J+1)-E(0,J), \tag{5}$$

respectively.

The distortion constant H_e is treated as a fixed parameter in the least-squares fit. It is calculated from HD by isotopic scaling, i.e.,

$$H_e(\mathrm{HT}) = (\mu_{\mathrm{HD}}/\mu_{\mathrm{HT}})^3 H_e(\mathrm{HD}), \tag{6}$$

where μ_i is the reduced mass of the molecule i and $H_e(\mathrm{HD}) = 2.1 \times 10^{-5}$ cm^{-1} (*7*). The adjustable parameters are the three vibrational band origins ν_1, ν_4, and ν_5; the four rotational constants B_0, B_1, B_4, and B_5; and the two centrifugal distortion constants D_e and β_e. In Table II we list the values of molecular parameters found from the least squares fit. The fitted transition frequencies as well as their deviations from the observed line positions are shown in the second and third columns of Table I, respectively.

Once the HT ground state molecular constants have been derived, they may be used to calculate the same line positions observed in the two previous Raman studies (*17, 18*) of HT. Table III summarizes how these calculated line frequencies compare with those determined by Edwards *et al.* (*17*) shown in the second column and with those of Veirs and Rosenblatt (*18*) shown in the last column. It is clear at once that our calculated line positions nearly reproduce those of Veirs and Rosenblatt (*18*) within their stated uncertainty, but differ systematically by up to 6.5 cm^{-1} from those of Edwards *et al.* (*17*), a deviation far outside the combined error estimates. This

TABLE II

HT Ground State Molecular Constants Found from a Least-Squares Fit to the Observed Line Positions of the 1–0, 4–0, and 5–0 Bands

Molecular Constant	Value[a] (cm^{-1})
ν_0	0.0[b]
ν_1	3434.8064(82)
ν_4	12801.966(8)
ν_5	15619.252(7)
B_0	39.7675(15)
B_1	38.1473(22)
B_4	33.4465(14)
B_5	31.9047(13)
D_e	$2.057(15)\times10^{-2}$
β_e	$-4.92(21)\times10^{-4}$
H_e	1.55×10^{-5} [c]

a) 95 percent confidence limits in units of the last digit are shown in parentheses.

b) Defined as zero reference energy.

c) Held fixed; calculated from Eq. (6).

TABLE III

Comparison of the "Raman Scattering Experiments"

Transition	This Work[a] (cm^{-1})	Edwards et al.[b] (cm^{-1})	Veirs et al.[c] (cm^{-1})
$S_0(0)$	237.866	237.927	-
$S_0(1)$	394.800	394.952	-
$S_0(2)$	549.267	549.670	-
$Q_1(0)$	3434.806	3428.370	3434.9
$Q_1(1)$	3431.568	3425.133	3431.6
$Q_1(2)$	3425.103	3418.671	3425.1
$Q_1(3)$	3415.438	3409.047	3415.6
$Q_1(4)$	3402.599	3396.397	3402.8

a) Calculated from the least-squares fitted molecular constants.

b) Ref. (17).

c) Ref. (18).

astonishingly large discrepancy of the Q_1 transition between Edwards *et al.* (*17*) and those of Veirs and Rosenblatt (*18*) and our own calculations suggests possibly some wavelength calibration error in the Raman studies of Edwards *et al.* (*17*). Consequently, we are forced to omit the work of Edwards *et al.* in what follows.

Figures 5 and 6 present a Birge-Sponer plot and a plot of B_v versus $v + (1/2)$, respectively. In both cases the data are well represented by straight lines yielding

$$\omega_e = 3590(1)\ \mathrm{cm}^{-1}$$

$$\omega_e x_e = 77.8(3)\ \mathrm{cm}^{-1}$$

and

$$B_e = 40.53(3)\ \mathrm{cm}^{-1}$$

$$\alpha_e = 1.571(7)\ \mathrm{cm}^{-1},$$

respectively. The standard deviations are in the parentheses with units of the last digit. The range of vibration covered is not large so that these parameters cannot be considered to be well known. Even if all ν_v and B_v values had been available, it is well known that an expansion in $v + (1/2)$ suffers convergence problems (*26*) and the values of the parameters (the so-called molecular constants) vary with the order of the fit. Nevertheless, it is interesting to compare the values of D_e, β_e, and H_e calculated in terms of the constants B_e, ω_e, $\omega_e x_e$, and α_e from theoretical formulae derived by Dunham (*27*) with those used in the least-squares fit. We find $D_e = 2.07 \times 10^{-2}\ \mathrm{cm}^{-1}$,

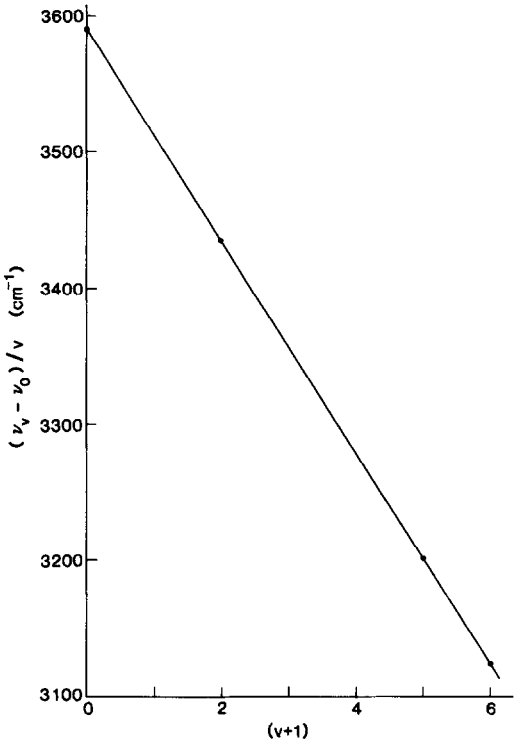

FIG. 5. Birge–Sponer plot of HT. The band origins are derived from the least-squares fit (see text and Table II). Note that the abscissa is in $(v + 1)$, and the intercept gives ω_e and the slope gives $-\omega_e x_e$.

$\beta_e = -5.4 \times 10^{-4}$ cm^{-1}, and $H_e = 1.51 \times 10^{-5}$ cm^{-1}, which nearly duplicate the corresponding values listed in Table II.

IV. DISCUSSION

With the advent of high-speed computers it is possible to solve the Schrödinger equation within the adiabatic approximation to a high degree of accuracy for the ground electronic state of H_2 and its isotopic analogs. Most of these advances are due to the pioneering efforts of Kołos and Wolniewicz, and an excellent review of such work prior to 1980 has been given by Bishop and Cheung (*30*). A recent such calculation is that of Hunt *et al.* (*31*) who provided in 1984 a table of $E(v, J)$ values for $v = 0$–5 and $J = 0$–5 for H_2, HD, D_2, HT, DT, and T_2. These calculations appear to include both relativistic corrections, as given by Kołos and Wolniewicz (*32*), and radiative corrections, as given by Bishop and Cheung (*33*). Table IV and V compare experimentally determined line positions for the 1–0, 4–0, and 5–0 bands in HD and HT with those predicted by Ref. (*31*). We note that the differences between the calculated and observed values are (1) comparable for HD and HT, (2) increase in a systematically positive manner with transition frequency (upper state v), and (3) exceed the experi-

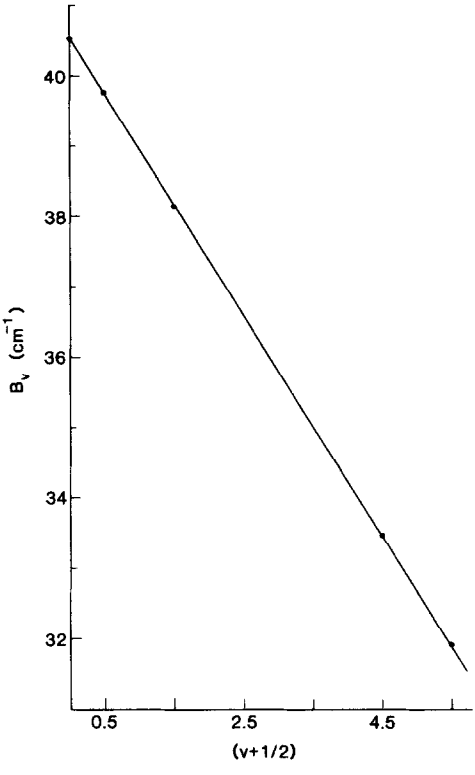

FIG. 6. A plot of B_v vs $[v + (1/2)]$ for HT. The B_v values are derived from the least-squares fit to the observed rotation-vibration line positions. (See text and Table II). The intercept gives B_e and the slope gives $-\alpha_e$.

mental error by several orders of magnitude. Thus, as realized some time ago (*30*), the adiabatic treatment is insufficient to describe the energy levels of molecular hydrogen.

Nonadiabatic effects involving the coupling between electronic and nuclear motions have been calculated for molecular hydrogen and its isotopic analogs by a number of workers. In particular, Wolniewicz (*34*) calculated in 1983 the energies of all bound vibrational states of H_2, HD, and D_2 with rotational quantum numbers up to $J = 5$. This calculation treats the nonadiabatic effects using variation-perturbation methods in which the zeroth-order function has the form of a product of the Born–Oppenheimer (clamped nuclei) electronic wavefunction times the adiabatic vibration–rotation wavefunction for the nuclear motion. Table VI compares these calculations with the observed line position for the 1–0, 4–0, and 5–0 bands of HD. We find that the inclusion of nonadiabatic effects reduces the differences between the calculated and observed line positions by more than a factor of 25 (see Table IV) but the remaining discrepancies are still larger than the experimental uncertainties. Wolniewicz (*34*) suggests that the accuracy of the nonadiabatic corrections is better than 0.01 cm^{-1}, i.e., better than 10 times the 4–0 and 5–0 line position differences. He attributes the

TABLE IV

Comparison of HD Experimental Line Positions with the Ab Initio Calculation without Nonadiabatic Corrections

Transition	ab initio Calc.[a] (cm^{-1})	Expt.[b),c)] (cm^{-1})	Calc.-Expt. (cm^{-1})
	1-0 Band		
$P_1(3)$	3356.007	3355.361	0.646
$P_1(2)$	3451.110	3450.463	0.647
$P_1(1)$	3543.590	3542.932	0.658
$R_1(0)$	3718.205	3717.532	0.673
$R_1(1)$	3799.132	3798.455	0.677
$R_1(2)$	3875.039	3874.357	0.682
$R_1(3)$	3945.409	3944.720	0.689
$R_1(4)$	4009.781	4009.088	0.693
	4-0 Band		
$P_4(2)$	13286.337	13283.993	2.344
$P_4(1)$	13390.002	13387.646	2.356
$R_4(0)$	13553.432	13551.065	2.367
$R_4(1)$	13612.035	13609.664	2.371
$R_4(2)$	13654.578	13652.215	2.363
$R_4(3)$	13680.683	13678.322	2.361
	5-0 Band		
$P_5(2)$	16222.261	16219.473	2.788
$P_5(1)$	16329.599	16326.791	2.808
$R_5(0)$	16489.356	16486.537	2.819
$R_5(1)$	16540.628	16537.816	2.812
$R_5(2)$	16572.207	16569.404	2.803
$R_5(3)$	16583.760	16581.008	2.752

a) Ref. (31). b) Ref. (13). c) Ref. (7).

major source of uncertainty in the calculation to the Born–Oppenheimer energy, which was performed more than 10 years earlier (*35–37*), and the relativistic correction. No comparable calculations have been carried out for HT of the nonadiabatic contribution to the energy levels.

However, stimulated by the Raman scattering studies of Veirs and Rosenblatt (*18*), Schwartz and Le Roy (*38*) have undertaken the task of producing a new compendium of vibration–rotation energy levels for all isotopes of molecular hydrogen. This is based on a slightly different Born–Oppenheimer potential curve of comparable accuracy with those of Ref. (*35–37*) and the systematic use of the accepted values of the nuclear masses. Because the relativistic and radiative corrections are independent of the in-

TABLE V

Comparison of HT Experimental Line Positions with the Ab Initio Calculation without Nonadiabatic Corrections

Transition	ab initio Calc.[a] (cm^{-1})	Expt.[b] (cm^{-1})	Calc.-Expt. (cm^{-1})
	1-0 Band		
$P_1(2)$	3273.781	3273.140	0.641
$P_1(1)$	3355.996	3355.355	0.641
$R_1(0)$	3511.685	3511.020	0.665
$R_1(1)$	3584.198	3583.530	0.668
$R_1(2)$	3652.548	3651.870	0.678
$R_1(3)$	3716.320	3715.630	0.690
$R_1(4)$	3775.136	3774.450	0.686
	4-0 Band		
$P_4(1)$	12724.787	12722.515	2.272
$R_4(0)$	12871.077	12868.786	2.291
$R_4(1)$	12924.826	12922.534	2.292
$R_4(2)$	12965.123	12962.825	2.298
$R_4(3)$	12991.657	12989.369	2.288
$R_4(4)$	13004.192	13001.917	2.275
	5-0 Band		
$P_5(2)$	15447.836	15445.118	2.718
$P_5(1)$	15542.532	15539.796	2.736
$R_5(0)$	15685.740	15682.984	2.756
$R_5(1)$	15733.339	15730.584	2.745
$R_5(2)$	15764.436	15761.691	2.745
$R_5(3)$	15778.752	15776.001	2.751

a) Ref. (31). b) This work.

dividual masses of the nuclei, they are combined with the Born–Oppenheimer potential to yield a mass-independent potential. Adiabatic corrections are calculated for H_2 using the method of Wolniewicz (*34*). Then adiabatic corrections are obtained for the other isotopes by scaling by $\mu(H_2)/\mu(i)$ where $\mu(i)$ is the reduced mass of the isotope. Nonadiabatic corrections for D_2 and T_2 are obtained from those for H_2 (*34*) and for HT and DT from HD (*34*) by suitable isotopic scaling. For a homonuclear molecule the nonadiabatic correction is

$$\Delta E_{na}(v,J) = \Delta E''(\Sigma_v) + J(J+1)A_v(\Pi_g), \tag{7}$$

and for a heteronuclear molecule

$$\Delta E_{na}(v,J) = \Delta E''(\Sigma_g) + \Delta E''(\Sigma_u) + J(J+1)[A_v(\Pi_g) + A_v(\Pi_u)], \tag{8}$$

TABLE VI

Comparison of HD Experimental Line Positions with Two Different Theoretical Calculations with Nonadiabatic Corrections

Transition	Expt.[a),b)] (cm^{-1})	ab initio[c)] - Expt. (cm^{-1})	Isotopic Scaling[d)] - Expt. (cm^{-1})
	1-0 Band		
$P_1(3)$	3355.361	0.026	0.011
$P_1(2)$	3450.463	0.018	0.002
$P_1(1)$	3542.932	0.019	0.002
$R_1(0)$	3717.532	0.018	0.001
$R_1(1)$	3798.455	0.012	-0.002
$R_1(2)$	3874.357	0.010	-0.003
$R_1(3)$	3944.720	0.010	-0.001
$R_1(4)$	4009.088	0.006	-0.003
	4-0 Band		
$P_4(2)$	13283.993	0.105	0.123
$P_4(1)$	13387.646	0.106	0.124
$R_4(0)$	13551.065	0.102	0.120
$R_4(1)$	13609.664	0.098	0.117
$R_4(2)$	13652.215	0.084	0.103
$R_4(3)$	13678.322	0.078	0.093
	5-0 Band		
$P_5(2)$	16219.473	0.123	0.145
$P_5(1)$	16326.791	0.132	0.154
$R_5(0)$	16486.537	0.128	0.150
$R_5(1)$	16537.816	0.113	0.137
$R_5(2)$	16569.404	0.100	0.125
$R_5(3)$	16581.008	0.046	0.071

a) Ref. (13). b) Ref. (7). c) Ref. (34). d) Ref. (38).

where Σ_g, Σ_u, Π_g, and Π_u identify the symmetries of states responsible. Isotope scaling is performed by multiplying $\Delta E''(\Sigma_g)$ by μ^{-1}, $A_v(\Pi_g)$ by μ^{-2}, $\Delta E''(\Sigma_u)$ by μ_α^{-1}, and $A_v(\Pi_u)$ by μ_α^{-2}, where μ is the reduced mass of the bare nuclei and $\mu_\alpha = m_1 m_2/(m_1 - m_2)$ and m_1 is the mass of the heavier isotope (bare nucleus). Finally, all vibration–rotation energies are lowered by 0.2 cm^{-1}, which is the convergence error of the Born–Oppenheimer potential as estimated by Wolniewicz (*34*).

The last column of Table VI lists the differences between the HD line positions found by Schwartz and Le Roy (*38*) and those experimentally determined by McKellar and co-workers (*7, 13*). For the HD 1–0 band the discrepancies appear to be smaller than those found using the calculations of Wolniewicz (*34*), but for 4–0 and 5–0 bands the discrepancies appear to be slightly larger for each transition studied.

TABLE VII

Comparison of HT Experimental Line Positions with Theoretical Calculations with Nonadiabatic Corrections

Transition	Isotopic Scaling[a] Calc. (cm^{-1})	Expt.[b] (cm^{-1})	Calc.-Expt. (cm^{-1})
	1-0 Band		
$P_1(2)$	3273.206	3273.140	0.066
$P_1(1)$	3355.410	3355.355	0.055
$R_1(0)$	3511.078	3511.020	0.058
$R_1(1)$	3583.581	3583.530	0.051
$R_1(2)$	3651.923	3651.870	0.053
$R_1(3)$	3715.687	3715.630	0.057
$R_1(4)$	3774.498	3774.450	0.048
	4-0 Band		
$P_4(1)$	12722.770	12722.515	0.255
$R_4(0)$	12869.038	12868.786	0.252
$R_4(1)$	12922.780	12922.534	0.246
$R_4(2)$	12963.071	12962.825	0.246
$R_4(3)$	12989.600	12989.369	0.231
$R_4(4)$	13002.132	13001.917	0.215
	5-0 Band		
$P_5(2)$	15445.446	15445.118	0.328
$P_5(1)$	15540.129	15539.796	0.333
$R_5(0)$	15683.317	15682.984	0.333
$R_5(1)$	15730.909	15730.589	0.320
$R_5(2)$	15762.002	15761.691	0.311
$R_5(3)$	15776.316	15776.009	0.307

a) Ref. (38). b) This work.

Table VII compares the Schwartz and Le Roy calculation for HT (*38*) with the line position measurements of this work, and the differences between the two are plotted in Fig. 7 with solid symbols. It is clear that the differences are systematically positive, and they show a small rotational dependence within each vibrational band but a very large vibrational dependence. On the average, the magnitude of the discrepancies is approximately 0.05 cm^{-1} for the 1–0 band, while those for the 4–0 and 5–0 bands are 0.24 and 0.32 cm^{-1}, respectively. The line position differences increase monotonically with vibrational quantum number and they far exceed the uncertainties in the experimental measurements.

This year, Kołos *et al.* (*39*) performed a formidable new Born–Oppenheimer potential curve calculation in an attempt to remove all the discrepancies between theo-

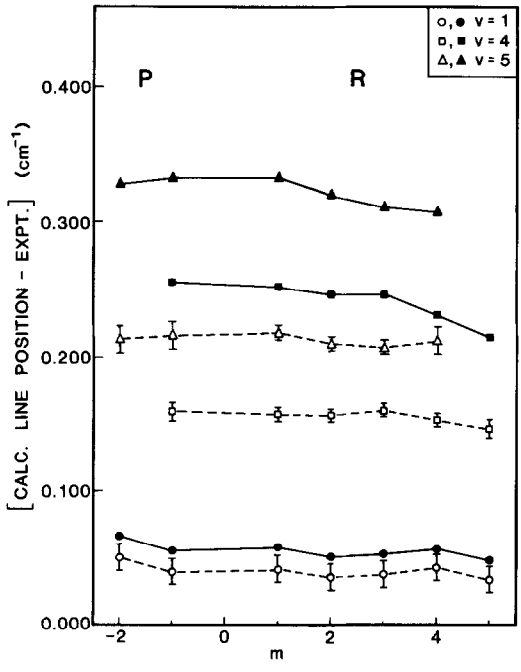

FIG. 7. HT line position differences, which represent the two sets of calculated values by Schwartz and Le Roy (*38, 43*) minus the observed value (this work), as a function of the index m. Here negative m values are for P-branch transitions ($J'' = -m$), positive values for R-branch transitions ($J'' = m - 1$), and $m = 0$ (missing line) is the band origin. The set of data with open symbols is improved over those with solid symbols by incorporating a more recent Born–Oppenheimer potential (*39*) (see text for details). The error bars represent only the uncertainties in the experimental line positions. For clarity error bars for the closed symbols are omitted. The straight line segments are drawn only as guides to the eye.

retical and experimental energy levels of the hydrogen molecule and its isotopomers in their ground electronic states. They recomputed the potential energy curve in the region $0.2 \leqslant R \leqslant 12.0a_0$ with a higher and more uniform accuracy: 249 terms were used for $R < 4.8a_0$ and 72 terms for larger distances. Nevertheless, they concluded with disappointment that in comparison with the H_2, HD and D_2 vibrational energy levels and the dissociation energies determined from emission measurements (*40–42*), there is hardly any improvement over the previous calculations (*34–37*).

It should be noted, however, that the emission measurements of Herzberg *et al.* (*40–42*) are not highly accurate due to the intrinsic limitations of those experiments. If we compare the HD vibrational origins of the newly improved calculation (*39*) with those derived from the more accurate absorption measurements (*7*), a dramatic reduction in discrepancies is obvious (see Table VIII). This result confirmed the suggestion by Wolniewicz (*34*) that the major error in the previous ab initio calculation arose from the inaccuracy of the old Born–Oppenheimer potential. We also believe that Kołos and his co-workers have demonstrated that the best ab initio calculation is capable of reproducing the energy levels of the low-lying rovibrational levels of the

ground electronic states of H_2, HD, and D_2 to within or close to the experimental uncertainties [see Ref. (*18*) for more detailed comparisons].

Using this newly improved Born–Oppenheimer potential, Schwartz and Le Roy (*43*) have recalculated the energy levels of HT from HD by isotopic scaling and by introducing an implicit J dependence into the rotationless $\Delta E''$ values [see Eqs. (7) and (8)]. The comparison of their updated calculation and the present experimental measurements is shown in Table IX and the differences are plotted in Fig. 7 with open symbols. For the two higher vibrational levels, there is approximately a 0.1-cm^{-1} reduction in the discrepancies between experiment and theory, but the mismatches are still far outside the experimental uncertainties.

It might be wondered whether pressure shifts in the experimentally determined line positions cause this disagreement. It should be recalled that no corrections were made for this effect because it was argued that the pressure shifts are comparable to or smaller than the measurement uncertainties.

Another factor that argues against the pressure effect being responsible for the differences between experiment and theory is the following. In order to cause the discrepancies between the experimentally measured HT 1–0 band transitions and the isotopically scaled ones to be comparable to those of HD, a pressure shift of −0.041 cm^{-1} must be assumed for these transitions. However, the pressure shifts increase almost linearly with vibrational quantum number (*13*) for the same pressure and they vary linearly with the gas pressure. Thus, for an assumed shift of −0.041 cm^{-1} for the 1–0 band, we estimate those for the 4–0 and 5–0 bands to be −0.197 and −0.410 cm^{-1}, respectively, based on our experimental conditions. Such corrections will bring

TABLE VIII

Comparison of HD Vibrational Origins

v	ν_v [a] (cm^{-1})	ab initio [b] − expt. (cm^{-1})	ab initio [c] − expt. (cm^{-1})	isotopic scaling [d] − expt. (cm^{-1})
1	3632.152(9)	0.027	0.008	-0.008
2	7086.887(41)	0.025	-0.010	-0.028
3	10367.608(8)	0.088	0.023	0.011
4	13467.872(8)	0.108	0.023	0.016
5	16416.021(9)	0.130	0.029	0.023
6	19185.220(27)	0.167	0.056	0.047

a) Ref. (7): experimental values. Numbers in parentheses are 3σ in units of the last digits.
b) Ref. (34).
c) Ref. (39).
d) Ref. (43).

TABLE IX

Comparison of HT Experimental Line Positions with Theoretical Calculations which Use a New Born–Oppenheimer Potential and Include Nonadiabatic Corrections

Transition	Isotopic Scaling[a] Calc. (cm^{-1})	Expt.[b] (cm^{-1})	Calc.-Expt. (cm^{-1})
	1-0 Band		
$P_1(2)$	3273.191	3273.140	0.051
$P_1(1)$	3355.395	3355.355	0.040
$R_1(0)$	3511.062	3511.020	0.042
$R_1(1)$	3583.566	3583.530	0.036
$R_1(2)$	3651.908	3651.870	0.038
$R_1(3)$	3715.673	3715.630	0.043
$R_1(4)$	3774.484	3774.450	0.034
	4-0 Band		
$P_4(1)$	12722.674	12722.515	0.159
$R_4(0)$	12868.943	12868.786	0.157
$R_4(1)$	12922.690	12922.534	0.156
$R_4(2)$	12962.985	12962.825	0.160
$R_4(3)$	12989.522	12989.369	0.153
$R_4(4)$	13002.063	13001.917	0.146
	5-0 Band		
$P_5(2)$	15445.331	15445.118	0.213
$P_5(1)$	15540.012	15539.796	0.216
$R_5(0)$	15683.202	15682.984	0.218
$R_5(1)$	15730.799	15730.589	0.210
$R_5(2)$	15761.898	15761.691	0.207
$R_5(3)$	15776.221	15776.009	0.212

a) Ref. (43). b) This work.

the discrepancies for the 4–0 band from ca. 0.15 cm^{-1} to ca. −0.04 cm^{-1} and those for the 5–0 band from ca. 0.21 cm^{-1} to ca. −0.20 cm^{-1}, which are totally unacceptable. Thus, we believe that the discrepancies shown in Table IX and plotted in Fig. 7 indicate the inaccuracies in the best theoretical treatment presently available for HT.

The differences between the observed HD and HT line positions and those calculated without nonadiabatic correction (Tables IV and V) show comparable discrepancies. In contrast, the comparison of the observed HD line positions with those calculated with nonadiabatic corrections (Table VI, VIII) shows better agreement than the com-

parison of the observed HT line positions with those calculated from nonadiabatic corrections determined from HD by isotope scaling (Table VII and IX). Therefore we speculate that the treatment of Schwartz and Le Roy may be less accurate because of their use of isotope scaling to estimate the nonadiabatic corrections to the HT vibration-rotation energy levels. A proper ab initio calculation of the nonadiabatic correction for HT is necessary to confirm or refute this speculation.

ACKNOWLEDGMENTS

This work benefitted significantly from the availability of the unpublished experimental work of K. Veirs and G. M. Rosenblatt and the unpublished theoretical work of C. Schwartz and R. J. Le Roy. We are grateful to these authors for sharing with us the results of their studies. We also thank the San Francisco Laser Center for the loan of equipment. Without this assistance, the present work never would have been accomplished. We also express our appreciation to C. G. Stevens who arranged for repeated shipments of tritium-containing samples from Lawrence Livermore National Laboratory and to the Stanford University Health Physics Department who monitored the safety of these studies. This work is supported in part by Amoco and by the National Science Foundation under NSF CHE 85-05926.

RECEIVED: February 3, 1986

REFERENCES

1. M. BORN AND R. OPPENHEIMER, *Ann. Phys.* **84**, 457–484 (1927).
2. M. BORN, *Nachr. Akad. Wiss. Göttingen* **6**, 1–3 (1951); M. BORN AND K. HUANG, "Dynamical Theory of Crystal Lattices," Oxford Univ. Press, New York, 1956.
3. R. L. WHETTEN, G. S. EZRA, AND E. R. GRANT, *Ann. Rev. Phys. Chem.* **36**, 277–320 (1985).
4. H. LEFEBVRE-BRION AND R. W. FIELD, "Perturbation in the Spectra of Diatomic Molecules," Academic Press, New York, in press.
5. B. P. STOICHEFF, *Canad. J. Phys.* **35**, 730–741 (1957).
6. U. FINK, T. A. WIGGINS, AND D. H. RANK, *J. Mol. Spectrosc.* **18**, 384–395 (1965).
7. A. R. W. MCKELLAR, W. GOETZ, AND D. A. RAMSAY, *Astrophys. J.* **207**, 663–670 (1976).
8. A. R. W. MCKELLAR AND T. OKA, *Canad. J. Phys.* **56**, 1315–1320 (1978).
9. P. J. BRANNON, C. H. CHURCH, AND C. W. PETERS, *J. Mol. Spectrosc.* **27**, 44–54 (1968).
10. D. E. JENNINGS AND J. W. BRAULT, *Astrophys. J.* **256**, L29–L31 (1982).
11. S. L. BRAGG, J. W. BRAULT, AND W. H. SMITH, *Astrophys. J.* **263**, 999–1004 (1982).
12. D. E. JENNINGS AND J. W. BRAULT, *J. Mol. Spectrosc.* **102**, 265–272 (1983).
13. N. H. RICH, J. W. JOHNS, AND A. R. W. MCKELLAR, *J. Mol. Spectrosc.* **95**, 432–438 (1982).
14. J. REID AND A. R. W. MCKELLAR, *Phys. Rev. A* **18**, 224–228 (1978).
15. V. DE COSMO, H. P. GUSH, AND M. HALPERN, *Canad. J. Phys.* **62**, 1713–1718 (1984).
16. P. LALLEMAND, P. SIMOVA, AND G. BRET, *Phys. Rev. Lett.* **17**, 1239–1241 (1966).
17. H. G. M. EDWARDS, D. A. LONG, H. R. MANSOUR, AND K. A. B. NAJM, *J. Raman Spectrosc.* **8**, 251–254 (1979).
18. K. VEIRS AND G. M. ROSENBLATT, *J. Mol. Spectrosc.* **121**, 401–419.
19. S. L. BRAGG AND W. H. SMITH, *Bull. Amer. Astron. Soc.* **9**, 516–517 (1977).
20. W. H. SMITH AND J. GELFAND, *J. Quant. Spectrosc. Radiat. Transfer* **24**, 15–17 (1980).
21. F. W. DALBY AND J. VIGUÉ, *Phys. Rev. Lett.* **43**, 1310–1314 (1979).
22. W. KOŁOS AND L. WOLNIEWICZ, *J. Chem. Phys.* **45**, 944–946 (1966); see, however, W. R. THORSON, J. H. CHOI, and S. K. KNUDSON, *Phys. Rev. A* **31**, 22–33, 34–42 (1985) for a different point of view.
23. G. C. WICK, *Atti. R. Acad. Naz. Lincei, Ser. 6* **21**, 708–714 (1935).
24. M.-C. CHUANG AND R. N. ZARE, *Chem. Phys. Lett.* **115**, 47–50 (1985).
25. H. M. CROSSWHITE, *J. Res. Nat. Bur. Stds.* **79A**, 17–69 (1975).
26. G. HERZBERG AND L. L. HOWE, *Canad. J. Phys.* **37**, 636–659 (1959).

27. J. L. DUNHAM, *Phys. Rev.* **41,** 721–731 (1932).
28. P. DION AND A. D. MAY, *Canad. J. Phys.* **51,** 36–39 (1973).
29. S. NAZEMI, A. JAVON, AND A. S. PINE, *J. Chem. Phys.* **78,** 4797–4805 (1983).
30. D. M. BISHOP AND L. M. CHEUNG, *Adv. Quantum Chem.* **12,** 1–42 (1980).
31. J. L. HUNT, J. D. POLL, AND L. WOLNIEWICZ, *Canad. J. Phys.* **62,** 1719–1723 (1984).
32. W. KOŁOS AND L. WOLNIEWICZ, *J. Chem. Phys.* **41,** 3663–3673 (1964).
33. D. M. BISHOP AND L. M. CHEUNG, *J. Chem. Phys.* **69,** 1881–1883 (1978).
34. L. WOLNIEWICZ, *J. Chem. Phys.* **78,** 6173–6181 (1983).
35. W. KOŁOS AND L. WOLNIEWICZ, *J. Chem. Phys.* **49,** 404–410 (1968).
36. W. KOŁOS AND L. WOLNEIWICZ, *Chem. Phys. Lett.* **24,** 457–460 (1974).
37. W. KOŁOS AND L. WOLNIEWICZ, *J. Mol. Spectrosc.* **54,** 303–311 (1975).
38. C. SCHWARTZ AND R. J. LE ROY, private communication.
39. W. KOŁOS, K. SZALEWICZ, AND H. J. MONKHORST, *J. Chem. Phys.* **84,** 3278–3283 (1986).
40. I. DABROWSKI, *Canad. J. Phys.* **62,** 1639–1664 (1984).
41. I. DABROSWKI AND G. HERZBERG, *Canad. J. Phys.* **54,** 525–567 (1976).
42. H. BREDOHL AND G. HERZBERG, *Canad. J. Phys.* **51,** 867–887 (1973).
43. C. SCHWARTZ AND R. J. LE ROY, *J. Mol. Spectrosc.* **121,** 420–439.